EXPERIMENTAL STUDIES OF BOUNDARY LAYER DYNAMICS USING ACTIVE FLOW CONTROL OF LARGE-SCALE STRUCTURES

Mitchell Lozier

Department of Aerospace and Mechanical Engineering
University of Notre Dame
Notre Dame, Indiana, 46556, USA
mlozier@nd.edu

Samaresh Midya

Department of Aerospace and Mechanical Engineering
University of Notre Dame
Notre Dame, Indiana, 46556, USA
smidya@nd.edu

Flint O. Thomas

Department of Aerospace and Mechanical Engineering
University of Notre Dame
Notre Dame, Indiana, 46556, USA
fthomas@nd.edu

Stanislav Gordeyev

Department of Aerospace and Mechanical Engineering
University of Notre Dame
Notre Dame, Indiana, 46556, USA
sgordeye@nd.edu

ABSTRACT

The dynamic response of a zero pressure gradient turbulent boundary layer (TBL) to a novel active flow control actuator was experimentally studied. The TBL has a relatively low Re-number, and does not have any discernable large-scale structure in the outer region. The periodically pulsed plasma actuator, placed inside the wake region of TBL, introduces a synthetic large-scale structure. Using a phase-locked analysis of the velocity across the boundary layer, it was found that the large-scale structure has a modulating effect on the turbulent structure in the near wall region, similar to the modulation that is observed in canonical TBLs at high Reynolds numbers.

INTRODUCTION

In recent years, the large-scale structures (LSS) in turbulent boundary layers (TBL) and their effect on technologically relevant flow properties (friction drag, noise, aero-optical distortions, flow separation etc.) have been extensively investigated [1,2,3] and it was unequivocally demonstrated that the dynamics of LSS and near-wall small-scale turbulence is correlated [3,4]. Furthermore, the influence of the LSS in TBL dynamics was shown to increase with Reynolds number [3].

In canonical boundary layers, thin shear layers, separating low-speed and high-speed regions (so-called uniform momentum regions), have been observed and studied in the last few years [5,6]. These thin shear layer structures, combined with the low momentum flow underneath them, are believed to be parts of a coherent structure, also known as the Attached Eddy. A more recent investigation of adverse pressure gradient TBLs demonstrated that the local flow physics is largely dominated by an embedded shear layer associated with the inflectional instability of the outer mean velocity profile inflection point [7]. Using scaling laws developed for free shear-layers but applied to the adverse pressure gradient (APG) TBL, profiles of mean velocity and turbulence quantities exhibited a remarkable collapse. The generic applicability of the embedded shear layer scaling was demonstrated by collapsing multiple APG turbulent boundary layer data sets from the AFOSR-IFP-Stanford Conference compiled by Coles and Hirst [8]. Further support for the influence of the shear layer structure on the near-wall TBL dynamics was recently provided by a study demonstrating that the presence of a free shear layer just outside a TBL has a significant effect on the near-wall burst/sweep events [9].

Collectively, the results described above strongly suggest that embedded shear layers are a generic feature of all TBLs irrespective of whether or not the mean velocity profile is inflectional. Although more apparent in APG boundary layers with inherent inflectional mean velocity profiles, transient and non-localized inflectional instabilities could well account for the enhancement of outer large-scale boundary layer structure that has been documented in previous studies of high Reynolds number zero pressure gradient TBLs. These shear-layer-like structures likely play an important role in determining LSS dynamics and ultimately in the global properties of the TBL.

An intriguing aspect of the presence of shear layers in the TBL is that they are very amenable to control. The ability to independently control outer layer LSS in the TBL offers new possibilities for uncovering their underlying dynamic. This aspect has been largely unexplored and most studies and models regarding the relationship between the small- and the large-scale structures deal with natural un-manipulated TBLs, and apply various conditional-averaging techniques to study their interactions [4]. Only a small number of studies have investigated modifying the LSS directly. In [10,11] an oscillating vertical plate was used to introduce a controlled traveling wave into the log-region of the boundary layer, and triadic interactions between the induced periodic structure and various scales in the boundary layer were studied. In [9] the turbulent boundary layer was externally forced by a shear layer and the turbulence inside the boundary layer was found to be both amplified and modulated by the external forcing.

Motivated, in part, by the results in [9], in this paper, active flow control is used to introduce periodic disturbances into the outer wake region of the turbulent boundary layer. The turbulent boundary layer Reynolds number is low enough that there is no naturally occurring outer large-scale structure present. By introducing periodic distortions, a synthetic large-scale structure was introduced into the boundary layer, and the boundary layer response to this structure was studied.

EXPERIMENTAL SET-UP

All of the experimental results presented in this paper were obtained using the 2' x 2' subsonic in-draft wind tunnel facility in the Hessert Laboratory at the University of Notre Dame. The overall dimensions of the tunnel test section are 2' x 2' x 7'. For this experiment, a 2 meter long boundary layer development

plate with a roughness element attached to the leading edge was installed into the test section. CTA anemometer with a single boundary layer hot-wire probe (Dantec Type 55P15) 5 μm diameter and l = 1.5 mm (l^+ =26) long was used to collect time series of the streamwise velocity component. The hot-wire was placed on a computer-controlled traverse system to position the hot-wire probe at different wall-normal locations. The traverse stage was inserted through the top wall of the tunnel along the middle of the tunnel span to allow a hot wire anemometer probe to be positioned at different streamwise locations. A plasma actuator, as described below, was attached to the boundary layer development plate at a fixed streamwise location of 140 cm from the leading edge of the boundary layer development plate. The experimental set-up with a plasma actuator, a hot wire probe and the coordinate system can be seen in Figure 1. A pitot probe was also inserted upstream of the plasma actuator through the side wall of the tunnel in order to measure the free stream velocity of the tunnel in order to calibrate the hot wire probe.

The plasma actuator, consisted of a thin rectangular plate and positioned parallel to the wall along the spanwise direction, was supported in the tunnel by two vertical NACA0010 airfoil supports 50 mm long and variable heights, H. The plasma actuator plate is W = 10 cm wide in the spanwise direction and L = 52 mm in the streamwise direction. The actuator plate was made from a 2 mm thick sheet of Ultem dielectric polymer. The leading edge of the actuator plate was rounded and the trailing edge was tapered to minimize the separation region behind the trailing edge of the plate. The alternating current (AC) plasma formed on the actuator was produced using a function generator, power amplifiers and a transformer [12]. Electrodes on the top and bottom of the actuator were connected to the high voltage AC source that provided a 40kV peak-to-peak sinusoidal waveform excitation to the electrodes at a frequency of 4 kHz. At this high actuation frequency, the plasma operates in a quasi-steady mode, essentially creating a steady jet. To introduce periodic forcing, a fifty percent duty cycle was imposed on the waveform, with a repetition frequency, f_p, which can be varied between 50 and 300 Hz.
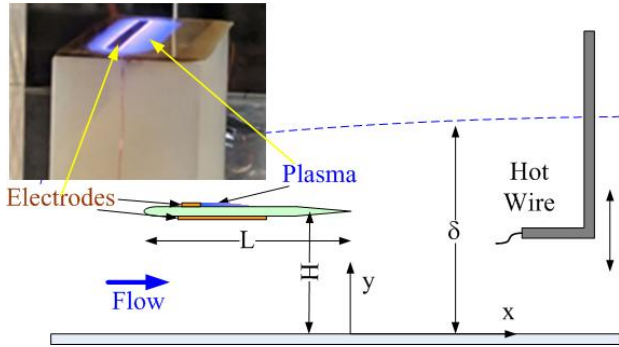

Figure 1. Schematic of the experimental set-up with a picture of the plasma actuator.

Hot wire voltages, pitot probe transducer voltages and the output of the function generator were recorded simultaneously. The velocity at each point was sampled at f_s = 30 kHz (corresponding to $\Delta t^+ = (1/f_s)u_\tau^2/\nu = 0.2$) for 120 seconds, or about 25,000 δ/U_∞. The hot wire probe was conditioned by a low pass filter with a cutoff frequency of 14 kHz to eliminate aliasing effects.

DATA REDUCTION

The measured voltages from the hot wire probe were converted into velocities, using a 3rd-order polynomial calibration. After the hot wire voltages were converted to velocities, the time mean, U, and root mean square (RMS) of the velocity, u_{rms}, were calculated at every point using standard methods.

Since the actuator introduced periodic forcing into the flow, it is convenient to phase-lock the results to the actuation frequency. To do so, a triple phase-locked Reynolds decomposition of the velocity was considered, as shown in Eq.(1),

$$u(y,t) = U(y) + \tilde{u}(y,\varphi) + u'(y,\varphi,n) \qquad (1)$$

where u is the instantaneous velocity, U is the time mean component of velocity, $\tilde{u}$ is a phase dependent or modal velocity component, u' is a residual fluctuating turbulent component, φ is the phase, defined by the relationship in Eq. (2), and n is the number of realizations as described below

$$t_n = \left(\frac{\varphi}{2\pi} + n\right)T_p \qquad (2)$$

Here t_n is a time in the nth realization, and is related to the phase angle, φ, by the period of the forcing repetition cycle, $T_p = 1/f_p$. The output of the function generator was used to ensure the data was phase locked with the repetition cycle of the plasma. These n realizations were then ensemble averaged to determine how the modal component of velocity varies as a function of the phase angle.

The remaining fluctuating component of the velocity, u', was used to quantify as ensemble-averaged RMS of the residual fluctuating turbulence,

$$u'_{rms}(y) = \left(\left\langle \left[u'(y,\varphi;n)\right]^2 \right\rangle_n\right)^{1/2} \qquad (3)$$

Here the $<\ >$ brackets denote ensemble averaging over all realizations. Later we will refer to this quantity as a residual turbulence level.

RESULTS

The baseline turbulent boundary layer characteristics at the measurement location were measured to ensure canonical behavior. These are summarized in Table 1. Skin friction velocity, u_τ, was determined using Clauser method.

Table 1. Boundary layer parameters

δ	U_∞	u_τ	C_f	H	Re_θ	Re_τ
33.2 mm	6.95 m/s	0.304 m/s	0.0039	1.368	1,770	683

The mean velocity of the boundary layer in the inner units, is presented in Figure 2. The universal fit for the log-region, $U^+ = 1/\kappa \ln(y^+) + C$, for values of κ = 0.385 and C = 4.1 is also plotted in Figure 2. The buffer and viscous sublayer can be seen below y^+ <30. The log region of the boundary layer is present between $40 < y^+ < 200$. The geometric center of the log-region is located appoximately at y+ ~ 90, very close to the expected value of $y_{OL}^+ \sim 3.9\,Re_\tau^{1/2} = 102$ [2,13].

The fluctuating energy component of the velocity, u'^2_{rms}, for the canonical boundary layer in the inner units is shown in Figure 3. The maximum turbulence level occurs at y+ = 15, with the value of $u'^2_{rms}/u_\tau^2 \sim 6.6$. The corresponding premultiplied energy spectrum is presented in Figure 4. Only the inner peak at $y^+ \sim 15$ and $\lambda^+ \sim 800$ is present in the energy spectra. The outer peak is essentially absent since in this experiment, Re_τ is relatively low.
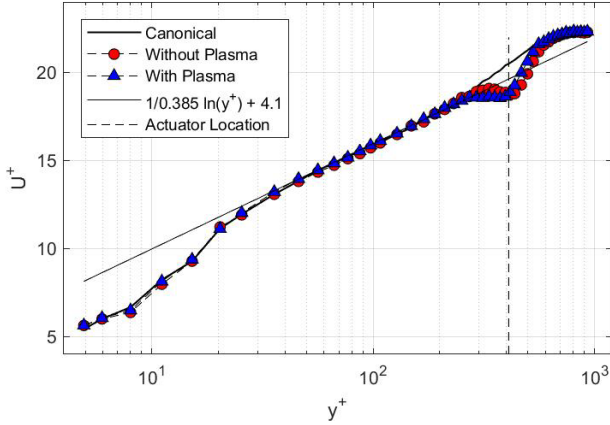

Figure 2. Mean velocity profile for the canonical boundary layer and for plasma off and periodic plasma on cases at x = 3δ downstream of plasma actuator. The actuator location is indicated by a vertical dashed line.
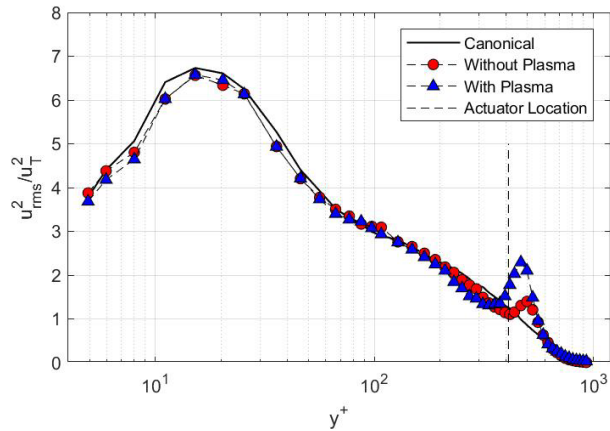

Figure 3. Normalized variance profiles for the canonical boundary layer and for plasma off and periodic plasma on cases at x = 3δ downstream of plasma actuator. The actuator location is indicated by a vertical dashed line.

The plasma actuator performance depends on two parameters: the excitation voltage and the repetition frequency. In order to characterize the authority of the plasma actuator, the first experiment was to examine the wake response downstream of the plasma actuator while it was in the freestream, well outside of the boundary layer. During this experiment the voltage of the plasma actuator was incrementally increased until a satisfactory level of authority was observed. The results presented here and throughout the paper were obtained with the plasma actuator operating at 40 kV.
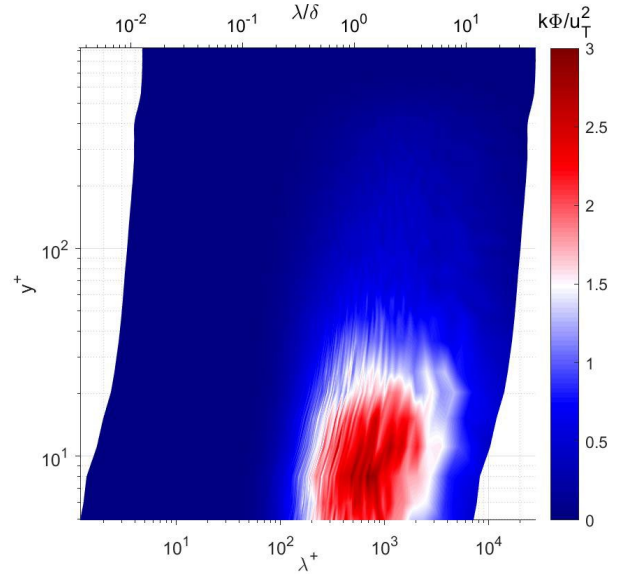

Figure 4. Pre-multiplied energy spectrum in the inner units for the canonical boundary layer at x = 3δ downstream of plasma actuator.

To establish an optimal actuation frequency, the repetition frequency was varied between 50 Hz and 300 Hz, and the mean velocity profiles were measured in the wake. The largest impact on the wake, characterized as a largest difference between plasma-off and periodic plasma-on cases, was observed at the low frequency of 50 Hz. At higher frequencies, the flow inertia, associated with the vortex formation in the wake, resulted in smaller velocity variations. Based on these studies, the repetition frequency of $f_p = 50$ Hz with 50% duty cucle was chosen for the boundary layer experiments. This frequency, if expressd in the boundary layer units, was $f_p\delta/U_\infty = 0.24$ and, in the inner units, $f_p^+ = 8 \times 10^{-3}$.

Once the effect of the plasma actuator in the uniform flow was investigated, it was placed inside of the boundary layer at a wall normal y-position of 0.6δ or $y_{act}^+ = 410$ away from the wall to measure the effect it had on the boundary layer. The actuator was positioned parallel to the wall along the spanwise direction with its trailing edge at x = 0. In the boundary layer units, the actuator was L = 1.5δ long in the streamwise direction, and W = 3δ wide in the spanwise direction. The velocity data were collected at two streamwise locations, x = 1.5δ and 3δ. The mean velocity profiles, U(y), in the boundary layer at x = 3δ for the case of plasma off and the periodic plasma on are presented in Figure 2, along with the velocity profile for the undisturbed canonical boundary layer. The mean velocity profiles for the canonical and plasma on and off cases show good agreement for $y^+ < 250$. As the plate is located approximately at $y_{act}^+ = 410$, indicated as a vertical dashed line in Figure 2, the velocity profile shows an actuation-related veclocity deficit in the wake region of the boundary layer between $200 < y^+ < 600$. Profiles of the normalized variance of the fluctuating velocity at x = 3δ for plasma off and plasma on cases are presented in Figure 3. The boundary layer statistics seems unchanged by the plasma actuator near the wall below for $y^+ < 200$. For the plasma off case, the small local increase in the turbulence levels, related to the turbulent wake downstream of the plate, can be observed between $400 < y^+ < 600$. Note that the local increaase in turbulence levels occur only above the plate, while the vairance is is slightly suppressed below the plate. When the periodic

plasma is turned on, the turbulent peak downstream of the plate widens and and is almost doubled in its intensity. Still, most of the increases in the turbulent intensity happens above the plate.

While the modifications of the mean and fluctuating velocity profiles in the wake region are a good indication that the actuator has authority in the boundary layer, the characterization of the interaction of an artificial or synthetic large-scale structure, introduced by the plasma actuator with the small scale turbulent structures near the wall is of a primary interest.

The pre-multiplied spectra at x = 3δ for the plasma on case is plotted in Figure 5. Compared to the pre-multiplied spectrum for the canonical boundary layer in Figure 4, the inner wall peak is largely unchanged by the operation of the actuator. The actuator introduces a periodic localized structure near $y^+ = 500$ with the characteristic length scale of $\lambda^+ =2{,}525$, or, in outer units, $\lambda =3.7\delta$.
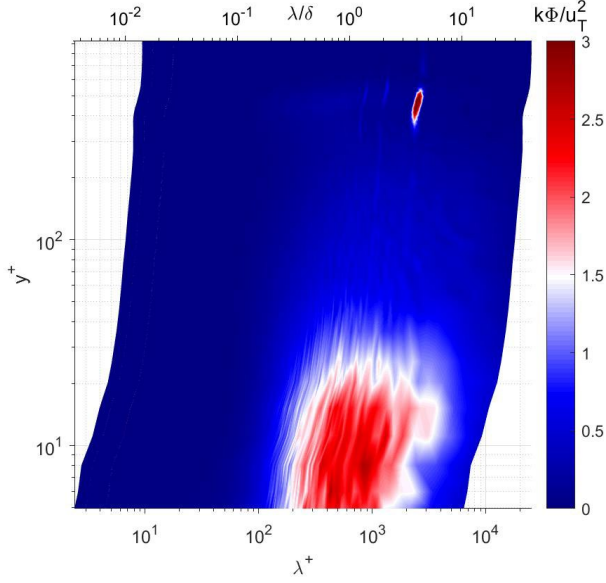

Figure 5. Pre-multiplied energy spectrum in the inner units for the plasma-on case at x = 3δ downstream of plasma actuator

Discerning the interaction between the outer large-scale and near-wall boundary layer structures is difficult by examination of only traditional time-mean velocity statistics and pre-multiplied spectra. In contrast, the triple decomposition, Eq. (1), allows one to study any potential phase-locking between the large-scale motion and the associated turbulence levels.

The phase-locked variation of the modal velocity component, $\tilde{u}(y,\varphi)$, associated with the synthetic large-scale structure was calculated. To visualize the actuator induced velocity field, the phase was converted into a pseudo-streamwise component using the frozen field assumption as, $x_{Pseudo} = -U(y)t = -U(y)(\varphi / 2\pi)T_p$, and the results of the measurements from two spatial locations, x = 1.5δ and x = 3δ, were blended together to create a pseudo-spatial map of the modal velocity which is presented in Figure 6. Large (on the order of u_τ) velocity deviations due to the combined effects from two shear layers, which form the wake, are present downstream of the actuator with alternating positive and negative values. The streamwise periodicity of the modal velocity is approximately 3.8δ. Above and below the actuator location, the modal velocity changes sign in the vertical direction; the locations of the sign change indicate the two shear layers. Closer to the wall, the velocity variations become smaller, but are still present.

The modal velocity in the inner units is presented as a function of phase in Figure 7. In the log-region between $40 < y^+ < 200$, the modal velocity has the negative excursions between 60 and 300 degrees, and the positive deviations elsewhere in phase. The amplitude of the modal velocity variations is about $0.2u_\tau$ in amplitude. These actuator-related variations in the modal velocity extend all the way into the viscous sublayer region. Thus, while not observable in the mean velocity profiles, the actuator does affect the local velocity throughout the log-region, buffer region and the viscous sublayer.
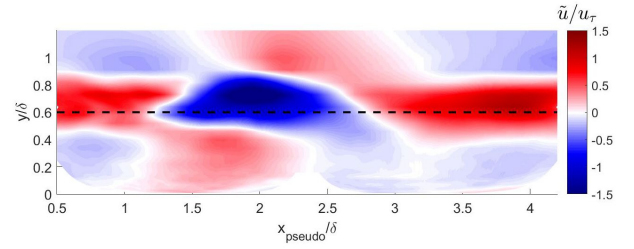

Figure 6. Pseudo-spatial map of the modal velocity downstream of the actuator, recreated using the Frozen Field assumption. The actuator y-location is indicated as a dashed line.
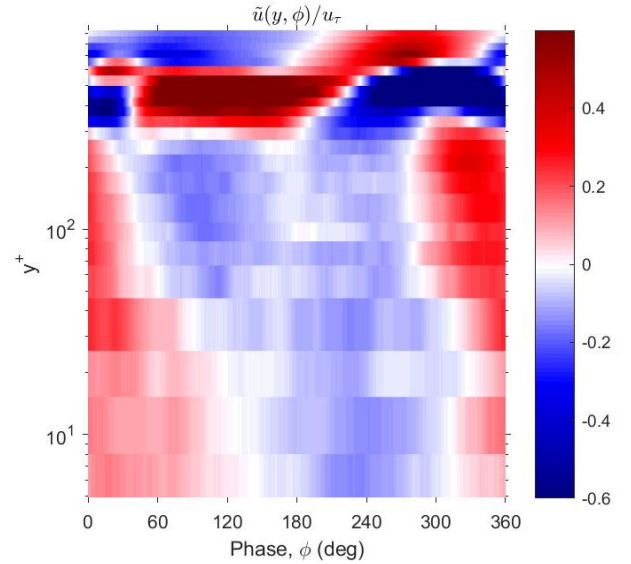

Figure 7. Modal velocity component, $\tilde{u}(y,\varphi)/u_\tau$, at x = 3δ downstream of the plasma actuator.

The phase-locked residual turbulence levels, u'_{RMS}, were also calculated for the periodic plasma on case. Since the changes in the residual turbulence level with the phase were small, compared to the time-averaged turbulence intensity, one way to present the results is to plot the mean-removed residual turbulence intensity,

$$\Delta u'_{rms}(y,\phi) = u'_{rms}(y,\phi) - \langle u'_{rms}(y,\phi) \rangle_\phi$$

This quantity is presented in Figure 8. Inside the plasma actuator induced wake, the turbulence varies significantly. The change over phase in $\Delta u'_{RMS}$ in the wake region happens because when the plasma is turned on the mean strain rate in the flow downstream of the actuator plate is increased and then relaxes back to its original state when the plasma is turned off. This fluctuating strain rate leads to fluctuating rates of turbulence

4

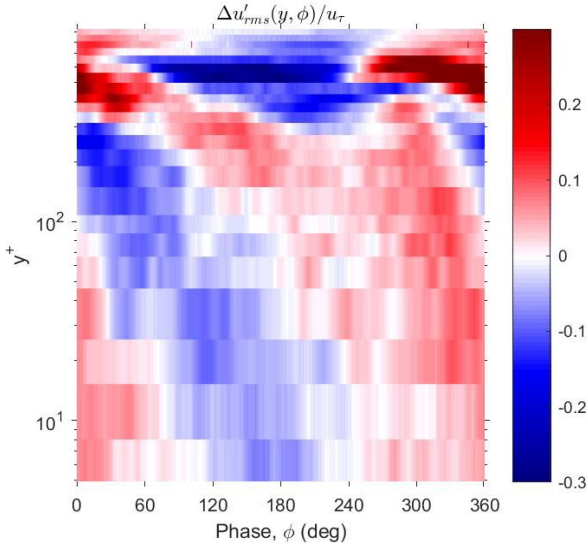production as the plasma is turned on and off during a single period.

Figure 8. The mean-removed residual turbulence intensity, $\Delta u'_{RMS}(y,\varphi)/u_\tau$ at x = 3δ downstream of plasma actuator.

Outside of the actuator-induced wake region, namely in the log-and the viscous sublayer region, the turbulence intensity is also affected, or modulated by the local changes in the modal velocity. The variations in the turbulence levels are on the order of $0.1u_\tau$; comparable to the amplitude variations in the modal velocity. In the log-region, the largest negative variations in the residual turbulence levels happen where the modal velocity has the largest negative gradient in phase; similarly, the largest positive values of $\Delta u'_{RMS}$ coincide with the phases where the modal velocity has the largest positive gradient. This correlation is expected as the turbulence production is proportional to $-\overline{\langle u'u'\rangle}\partial\tilde{u}/\partial x$ [14]. From Taylor's 'frozen' field hypothesis, it follows that, $\partial u/\partial x = -(1/U)\,\partial u/\partial t \sim \partial u/\partial\phi$. Thus, the turbulence production should be the largest where the temporal (i.e. phase) derivative of the local modal velocity is positive and vice versa, in accordance with the experimental observations. In the near-wall region, $y^+ \sim 10$, the turbulence intensity variations tend to become in phase with modal velocity fluctuations, in agreement with the quasi-steady model [15].

Thus, the synthetic large-scale structure, introduced by the actuator, clearly has a modulating effect on the boundary layer turbulence. To examine the modulation effect, Mathis et al [2] introduced a so-called R-coefficient which reflects the normalized correlation between the large-scale fluctuations and the properly filtered envelope of the small-scale turbulence. To separate the large- and the small-scale components of the velocity signal, they relied on the scale separation; that is, for sufficiently large Re_τ-numbers, the outer peak in the energy spectrum can be separated from the inner peak using a fixed length cut-off criterion. In the case of the internally forced boundary layer, studied in [10,11], the authors also relied on the separation of scales to isolate the large-scale structure induced by the forcing and the small-scale structures near the wall.

This approach is not directly applicable for the present data, since in this experiment there is no clear separation in scale between the near-wall structures and the synthetic plasma induced large-scale structure. This is apparent from the comparable wavelenghts of the inner and outer peaks shown in

Figure 5. Instead, we will use the fact that when using the triple phase-locked decomposition, we have already separated the effects of the synthetic large-scale structure, reflected in the modal velocity, $\tilde{u}$, from the resulting variations of an envelope in turbulence amplitude, given in $\Delta u'_{RMS}$. Therefore, similar to the R-coefficient definition, we can introduce a modulation coefficient, $\Phi(y)$, between the modal velocity and the (mean-removed) variations in residual turbulence amplitude, as given in Eq. (4),

$$\Phi(y) = \frac{\left\langle \tilde{u}(y,\phi)\Delta u'_{rms}(y,\phi)\right\rangle_\phi}{\sqrt{\left\langle \tilde{u}(y,\phi)^2\right\rangle_\phi}\sqrt{\left\langle \Delta u'_{rms}(y,\phi)^2\right\rangle_\phi}} \qquad (4)$$

where the angle brackets indicate ensemble averaging over all the phase angles. This Φ-coefficient was used to study the modulation effect in the externally forced turbulent boundary layer [9] and it was found to provide similar correlation results as the traditional R-coefficient.

Using the data shown in Figure 7 and Figure 8 the Φ-coefficient was calculated and is shown in Figure 9 as solid symbols. There is a relatively strong, $\sim 0.3..0.5$, positive correlation of the small-scale turbulent structures and the actuator-induced modal velocity in the near wall region, including the viscous sublayer region and the portion of the log-region up to $y^+ \sim 100$. Above this location, the variations in Φ-coefficient are primarily due to the actuator-induced wake, where the correlation is positive below the actuator plate and becomes negative above it.
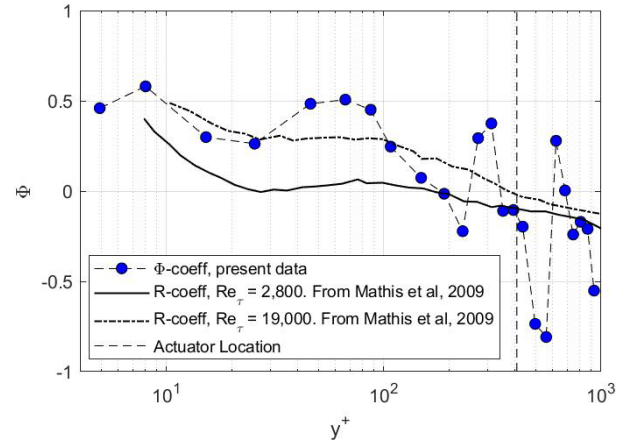

Figure 9. Modulation Φ-coefficient for periodic plasma on case at x = 3δ downstream of plasma actuator. The actuator location is indicated by a vertical dashed line. For comparison, R-coefficients for the canonical boundary layers for low Re_τ = 2,800 and high Re_τ = 19,000 from Mathis et al. [2] are also presented.

As mentioned before, the Φ-coefficient is expected to give similar correlation results as the R-coefficient. The R-coefficient for a canonical boundary layer with a relatively low, but similar to the present experiment, Re_τ = 2,800 from [2] is plotted in Figure 9 as a solid line. The R-coefficient also is positive in the viscous sublayer, y+ < 10, and it essentially zero everywhere else. Overall, the R-coefficient has consistently lower values than the Φ-coefficient. However, it is important to recognize that the boundary layer with periodic plasma actuation in the present experiment, while technically having a low Re_τ-value, is not a canonical boundary layer since the synthetic large-scale

structure was artificially introduced in the boundary layer. It would therefore be more appropriate to compare the Φ-coefficient results with the R-coefficient for a canonical boundary layer with high Re_τ, where the large-scale structure is naturally present. In [2] it was observed that the R-coefficient tends to increase in the region near the wall, $y^+ < 200$, due to an increased strength of the naturally occurring large-scale structure. The R-coefficient for high $Re_\tau = 19,000$ from [2] is also presented in Figure 9 as a dashed-dotted line. The agreement between high-Re R-coefficient and Φ-coefficient is much better. This result can be interpreted as the near-wall region responding to the artificially introduced large-scale structure in a similar manner as in the naturally occurring high Re boundary layer.

This result is very encouraging, as it proposes an alternative means to study the relevant boundary layer dynamics. Note that the passive presence of the actuator plate weakens the existing large-scale structure by eliminating vertical motions [16,17]. The weakened large-scale structure can then be "replaced" with an artificial actuator-controlled one. By placing this artificial large-scale structure at different wall-normal locations, the near-wall responce can be systematically studied and the current models of the boundary layer interactions can be updated.

CONCLUSIONS

From the experimental results, it has been shown that a periodic-pulsing plasma actuator placed inside of a turbulent boundary layer with relatively low Re-number introduces a synthetic large-scale outer structure, which alters the turbulent dynamics of the boundary layer. It has also been demonstrated that the plasma actuator has sufficient authority to modify both the mean velocity and *rms* velocity profiles of the boundary layer, and to produce phase dependent velocity fluctuations. Performing a phase-locked triple decomposition, it has been shown that the phase dependent velocity changes associated with the synthetic large-scale structure have a modulating effect on the amplitude of small-scale near-wall turbulent structures. A modulation coefficient, $\Phi(y)$, is defined which captures the degree of correlation between the actuator induced phase dependent fluctuations and those associated with near-wall turbulence. This is similar to the traditional modulation R-coefficient, applied in high Reynolds number canonical turbulent boundary layers. The results show that the near-wall region of the artificially forced low-Re boundary layers behaves in a similar fashion as the canonical boundary layer at high Re-number. These results suggest an aletrnative way to study the turbulent boundary layer dynamics by introducing a synthetic, periodic large-scale structure into different regions of the boundary layer and quantifying the overall responce of the boundary layer.

REFERENCES

[1] M Guala, SE Hommema, RJ Adrian, "Large-scale and very-large-scale motions in turbulent pipe flow," J. Fluid Mech. 554, pp. 521-542, 2006.

[2] Mathis, R., Hutchins N., and Marusic, I., "Large-scale Amplitude Modulation of the Small-scale Structures in Turbulent Boundary Layers." J. Fluid Mech. 628 (2009): 311-336.

[3] N. Hutchins and I. Marusic, "Large-scale influences in near-wall turbulence," Phil. Trans. R. Soc. A, 365, pp. 647–664, 2007.

[4] R. Mathis, N. Hutchins, and I. Marusic, "A predictive inner–outer model for streamwise turbulence statistics in wall-bounded flows," J. Fluid Mech., 681, pp. 537–566, 2011.

[5] Adrian, R. J., Meinhart, C. D. and Tomkins, C. D., "Vortex organization in the outer region of the turbulent boundary layer," J. Fluid Mech., 422, pp. 1-53, 2000.

[6] de Silva, C. M., Hutchins, N. & Marusic, I., "Uniform momentum zones in turbulent boundary layers," J. Fluid Mech., 786, pp. 309-331, 2016.

[7] D.M. Schatzman, and F.O. Thomas, "An experimental investigation of an unsteady adverse pressure gradient turbulent boundary layer: embedded shear layer scaling," J. Fluid Mech., 815, pp. 592–642, 2017.

[8] Computation of Turbulent Boundary Layers--1968 AFOSR-IFP-Stanford Conference: Compiled data. Editors: D. E. Coles and E. A. Hirst, Thermosciences Division, Stanford University, 1969.

[9] P. Ranade, S. Duvvuri, B. McKeon, S. Gordeyev, K. Christensen, and E.J. Jumper, "Turbulence Amplitude Amplification in an Externally Forced, Subsonic Turbulent Boundary Layer", to appear in AIAA J, 2019.

[10] Duvvuri, S., and McKeon, B.J., "Triadic Scale Interactions in a Turbulent Boundary Layer." J. Fluid Mech. 767, R4, 2015.

[11] Duvvuri, S., and McKeon, B., "Phase relations in a forced turbulent boundary layer: implications for modelling of high Reynolds number wall turbulence". Philos Trans A Math Phys Eng Sci., 375(2089), 20160080, 2017.

[12] Thomas, F. O., Corke, T. C., Iqbal, M., Kozlov, A. and Schatzman, D., "Optimization of SDBD Plasma Actuators for Active Aerodynamic Flow Control" AIAA J, 47(9), pp. 2169-2178, 2009.

[13] Klewicki, J., Fife, P., Wei, T. and McMurtry, P., "A physical model of the turbulent boundary layer consonant with mean momentum balance structure", Phil. Trans. R. Soc. Lond. A, 365, pp. 823–840, 2007.

[14] Reynolds, W.C. and Hussain, A.K.M.F. "The mechanics of an organized wave in turbulent shear flow. Part 3. Theoretical models and comparisons with experiments", J. Fluid Mech. Vol. 54, pp. 263–288, 1972.

[15] Zhang C, Chernyshenko SI., "Quasisteady quasihomogeneous description of the scale interactions in near-wall turbulence", Phys. Rev. Fluids 1, 014401, 2016.

[16] Corke TC, Guezennec YG and Nagib HM. "Modification in drag of turbulent boundary layers resulting from manipulation of large-scale structures." In Proc. Viscous Drag Reduction Symp., Dallas. AIAA Prog. Astro. Aero. 72, pp. 128-143, 1979.

[17] Bandyopadhyay, P.R. "Review - Mean flow in turbulent boundary layers disturbed to alter skin friction." Trans.ASME J. Fluids Engng 108, 127-140, 1986.